Journal of Power Sources 191 (2009) 534–541

Contents lists available at ScienceDirect

Journal of Power Sources

journal homepage: www.elsevier.com/locate/jpowsour

The effect of H_2S on the performance of Ni–YSZ anodes in solid oxide fuel cells

Jens F.B. Rasmussen, Anke Hagen*

Risø-DTU, Fuel Cells and Solid State Chemistry Division, Frederiksborgvej 399, DK-4000 Roskilde, Denmark

ARTICLE INFO

Article history:
Received 25 November 2008
Received in revised form 27 January 2009
Accepted 1 February 2009
Available online 7 February 2009

Keywords:
SOFC
Sulfur
Poisoning
Hydrogen sulfide
Biogas

ABSTRACT

Biomass-derived fuel, e.g. biogas, is a potential fuel for solid oxide fuel cells (SOFCs). At operating temperature (~850 °C) reforming of the carbon-containing biogas takes place over the Ni-containing anode. However, impurities in the biogas, e.g. H_2S, can poison both the reforming and the electrochemical activity of the anode.

Tests of single anode-supported planar SOFCs were carried out in the presence of H_2S under current load at 850 °C. The cell voltage dropped as we periodically added 2–100 ppm H_2S to an H_2-containing fuel in 24 h intervals, but it regenerated to the initial value after we turned off the H_2S. Evaluation of the changes of the cell voltage suggests that saturation coverage was reached at approximately 40 ppm H_2S. A front-like movement of S-poisoning over the anode was seen by monitoring the in-plane voltage in the anode. Furthermore, impedance spectra showed that mainly the polarization resistance increased when adding H_2S. These changes in resistance were found to happen at 1212 Hz, which is related to reactions at the anode–electrolyte interface. These findings can be used to identify S-related effects on the performance, when an SOFC is fuelled with biogas or other fuels with H_2S impurities and thus help in the development of more sulfur tolerant SOFCs.

1. Introduction

Biogas is a potential, direct fuel for solid oxide fuel cells (SOFCs). The Ni in the anode support and anode of a typical anode-supported SOFC acts as a reforming catalyst, converting CH_4 with steam to CO and H_2 which in turn are electrochemically converted to H_2O and CO_2. When using biogas directly without extensive purification, the concentration of impurities and their effects on the SOFC performance have to be considered. Among these impurities H_2S is very important. S-compounds are known to interact with Ni catalysts and passivate the active sites [1–3]. It is therefore necessary to study the fundamentals of how, and at what concentrations H_2S in the fuel affects the SOFC, in order to identify the poisoning mechanisms and to suggest means to increase the tolerance to S.

Several research groups have experimentally studied the effect of an S-containing fuel on performance and durability of an SOFC by varying several factors, such as for example the temperature, current/voltage load, time and H_2S concentration (0.02–240 ppm). Different SOFC systems were used in these studies: pellets, half-cells, full planar-SOFCs and stacks, but all had a Ni–YSZ (Nickel–Yttria-stabilized-Zirconia) cermet as anode material [4–12]. The general picture from these studies is that the performance of the SOFC degrades (with varying magnitude) when H_2S is added to an H_2 containing fuel, as an effect of the already mentioned S poisoning of the active sites on the Ni catalysts. The performance degradation was a result of an increase of the internal resistance of the SOFC and was reported as a two step process, i.e. an initial voltage drop followed by a constant voltage or a voltage degradation/increase, depending on the test parameters [8,11]. The reversibility of this process depended on the H_2S concentration. Zha et al. [11] found that a single SOFC with a Ni–YSZ cermet anode which had been exposed to a fuel containing 50 ppm H_2S at 800 °C, recovered 96% of its initial performance 50 h after stopping the H_2S exposure, whereas the recovery was 99% for 2 ppm H_2S. Cheng et al. [9] studied this performance loss further, by having H_2S (~0.2–10 ppm) in the $H_2/H_2O/N_2$ fuel of electrolyte supported SOFCs. The relative increase in internal cell resistance decreased with increasing current under either potentiostatic or galvanostatic conditions. Matsuzaki and Yasuda [4] found that reducing the operation temperature increased the effect of poisoning. The concentration of H_2S in the H_2/H_2O fuel to yield a detectable effect was found to be 2 ppm, 0.5 ppm and 0.05 ppm at 1273 K, 1173 K and 1023 K, respectively. Rostrup-Nielsen et al. [12] studied the effect of 10 ppm and 50 ppm H_2S in an SOFC 10-cell stack fuelled with a gas mixture simulating the composition of a jet and diesel fuel after catalytic partial oxidation in a Catator CPO (catalytic partial oxidation) unit (H_2, CO, CO_2, CH_4 and N_2). Adding 50 ppm H_2S at 700–720 °C resulted in a 10% decrease in voltage. When extra H_2 was submitted to the fuel an almost complete recovery of the voltage loss was

* Corresponding author. Tel.: +45 46 77 58 84; fax: +45 46 77 58 58.
E-mail address: anke.hagen@risoe.dk (A. Hagen).

0378-7753/$ – see front matter © 2009 Elsevier B.V. All rights reserved.
doi:10.1016/j.jpowsour.2009.02.001

achieved. The measurements illustrated that the CH_4 passed the stack nearly unconverted and thus that the CH_4 conversion is more sensitive to S-poisoning than the electrochemical reactions.

To minimize or at best eliminate these negative effects of S, S-tolerant materials have been studied both experimentally and theoretically [8,10,13–17]. Ce, Cu and Sc are among the materials that have been reported to increase the S tolerance of an SOFC. For example Sasaki et al. [8] found that the S-tolerance was improved by using Sc_2O_3-doped ZrO_2 (SSZ) instead of Y_2O_3-doped ZrO_2 (YSZ) as electrolyte and/or as electrolyte component in the anode cermet, when testing planar electrolyte-supported SOFCs. At 800 °C and a current density of 200 mA cm^{-2}, the cell voltage of an SOFC with a Ni–YSZ anode dropped to 0 V, when 20 ppm H_2S was added to the H_2 fuel, while an SOFC with a Ni–SSZ anode only experienced a small drop in voltage and continued to run even after 100 ppm H_2S was added.

In general though, it is difficult to find an unambiguous explanation for the reactions of S-compounds in the anode and the effects on performance, as it is very complex and dependant on the various factors already mentioned (e.g. temperature, H_2S concentration, fuel composition and operation time). However, it seems to be generally accepted that at least two different types of reactions can take place on the Ni catalyst particles, i.e. a chemisorption (Reaction (1)) and a sulfidation (Reaction (2) + (3)) [18,19].

$$H_2S(g) \leftrightarrow HS_{ads} + H_{g/ads} \leftrightarrow S_{ads} + H_{2,g/ads} \quad (1)$$

$$Ni + H_2S \leftrightarrow NiS + H_2 \quad (2)$$

$$3Ni + xH_2S \leftrightarrow Ni_3S_x + xH_2 \quad (3)$$

which of these reactions is dominating, has been studied theoretically (e.g. thermodynamical calculations) and experimentally (e.g. X-ray diffraction (XRD) and Raman spectroscopy) [19–23]. These studies indicated that chemisorption (Reaction (1)) is dominating at relevant testing conditions for an SOFC (700–800 °C and an H_2S concentration below ~50 ppm). Cheng and Liu [23] used in situ Raman spectroscopy to study dense Ni–YSZ composite pellets exposed to higher H_2S concentrations. Sulfides were only detected after cooling down slowly from 500 °C and they disappeared again after re-heating to over 500 °C. These results illustrate the problems of detecting sulfur by post-mortem analysis.

This paper presents experimental studies on the effect of H_2S added at intervals with different concentrations to an H_2 fuel on the performance of technological SOFCs with a Ni–YSZ anode cermet. Detailed electrical measurements and impedance spectroscopy were used to monitor the effect of S on the cell voltage and the internal resistance of the SOFCs. Scanning electron microscopy (SEM) and energy dispersive spectroscopy (EDS) were used to study the chemical composition and eventual morphology changes of the anode after the test.

2. Experimental

2.1. Cells and initial electrochemical characterization

The SOFCs consisted of a Ni/Yttria-stabilized-Zirconia (YSZ) anode support and an active Ni/YSZ anode, a YSZ electrolyte, and a Lanthanum–Strontium–Manganate (LSM)/YSZ cathode and were produced at the *Risø-DTU* pre-pilot facility [24,25]. The SOFCs were planar with an active area of 4 cm × 4 cm (total area of 5 cm × 5 cm). The cells were sandwiched, firstly, between an anode and a cathode gas distribution layer, and secondly, between current collectors, i.e. a Ni foil on the anode side and an Au foil on the cathode side. These components were all sealed from the surroundings by a glass/ceramic-composite. A more detailed description of the setup can be found in Ref. [26].

The cells were sealed and reduced at 1000 °C followed by an initial electrochemical characterisation (fingerprint). The fingerprint measurements comprised of iV-curves and impedance spectra at 850 °C, 800 °C and 750 °C in 96% H_2 + 4% H_2O and 80% H_2 + 20% H_2O fuel composition. In the impedance measurements an oscillating current of approximately 60 mA was applied over the frequency range 0.08–82 kHz with a *Solartron* impedance analyser.

2.2. The effect of H_2S

The effect of H_2S was measured with the setup shown in Fig. 1. The fuel consisted of H_2, which was moisturized in a water bottle (~4% H_2O). H_2S from an H_2S/H_2-bottle containing 218 ppm H_2S was supplied through a mass flow controller and mixed with the fuel after the water bottle, while the total fuel flow was kept constant at 10 l h^{-1}. The right-hand side of Fig. 1 illustrates how the H_2S was added at intervals. The exposure time was 24 h for each H_2S concentration. Air was used on the cathode side (140 l h^{-1}). The test was compared to an SOFC tested at similar test conditions, where the fuel was an H_2:CO_2 gas mixture (4:1) at a total flow of 12.5 l h^{-1}. The experimental schematic for the H_2S-poisoning tests was thus:

1. Adjustment of gas flows (anode: H_2/H_2O; cathode: air; start of current load (1 A cm^{-2}).
2. Waiting for a constant cell voltage (~200 h).
3. Addition of H_2S to the fuel flow for 24 h.
4. Stop of H_2S flow and waiting for cell voltage regeneration (~200 h).
5. Repetition of the H_2S addition for several different H_2S concentrations (2–100 ppm).
6. Cell voltage measurements during the entire test.
7. Impedance measurements at selected times.

In the fuel inlet and outlet tubes, pO_2 probes were placed to measure the oxygen partial pressure voltage (pO_2-in voltage and pO_2-out voltage, respectively). The pO_2 probes were made of single ended zirconia based tubes, and were supplied with a constant flow

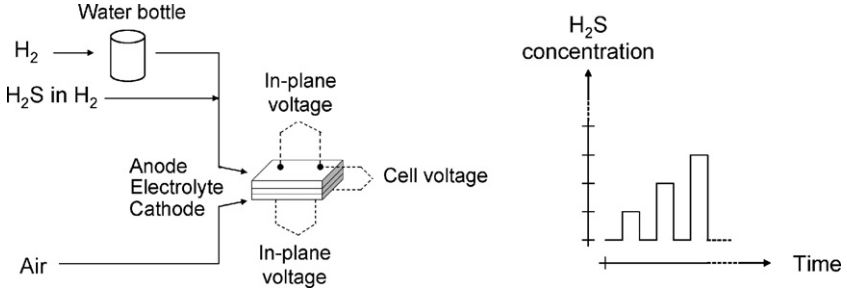

Fig. 1. The test setup. On the right it can be seen how H_2S was added at intervals.

of air on the inside. Two Pt wires (one on the inside and one on the outside of the tube) measure the potential difference across the tube wall. With use of Nernst equation the partial pressure of oxygen on the outside (the fuel) could be calculated as it is known on the inside (air). A third Pt/Rh wire was welded together with the inside Pt wire, and was used to measure the inlet and outlet fuel temperature.

The SOFC performance during the test was evaluated by measuring the cell voltage and the in-plane voltages in anode and cathode (see Fig. 1) as well as by impedance spectroscopy. These voltage measurements were carried out by using Pt voltage probes, which were welded onto the anode and cathode current collectors at the positions of gas inlet and outlet (see Fig. 1).

SEM/EDS were used post-test to study the effect of S on the chemical composition and morphology of the SOFC. For the SEM/EDS analysis 10 mm × 5 mm samples were broken off the SOFCs at the positions of gas-in and gas-out during testing. The samples were vacuum embedded into epoxy cylinders, so that their cross-section was aligned with the cylinder surface. The samples' cross-section was first grinded with SiC paper, secondly polished with diamond suspensions (minimum grain size of 1 μm). A carbon layer coating was put on top of the grinded surface.

3. Results

3.1. Performance

Two tests were performed on nominally identical cells, denoted as *H_2S test* and *reference test*. During the initial fingerprint the area specific resistance (*ASR*) values were obtained at 850 °C. For the *H_2S test* the *ASR* value was 0.16 Ω cm^2, while for the *reference test* it was 0.14 Ω cm^2. After the initial characterization, a current load of 1 A cm^{-2} was applied on the cell in the *H_2S test* at a total fuel flow of 10 l h^{-1} and a temperature of 850 °C. The initial cell voltage was 676 mV. The fuel utilization was ∼70% as measured by the pO_2 sensors. In the *reference test* the cell was fuelled with an H_2/CO_2 (4:1) gas mixture at 850 °C, with a current load of 1 A cm^{-2} and a fuel utilization of ∼65%. The cell voltages as a function of time for the two tests are shown in Fig. 2. The reference cell is seen to have a higher cell voltage (749 mV) than the cell in the *H_2S test* within the first 100 h. During the ∼1000 h period the cell voltage was very stable and only degraded by 6 mV. In the *H_2S test*, an initial increase of the cell voltage (activation) occurred to a value of 738 mV during the first 50 h, and thus increased to approximately the same cell voltage as for the reference cell. After approximately 200 h with a constant cell voltage, 2 ppm H_2S was added to the fuel. An effect (drop of cell voltage) occurred first after 18 h. This retention time is believed to be due to the fact that the pipes and various surfaces through the test setup had to be covered with S before the H_2S reached the cell. 24 h after the cell voltage started to drop the H_2S was turned off. This gave rise to a slow increase in the cell voltage over a period of approximately 250 h. This process was repeated several times with different H_2S concentrations added for 24 h. The initial retention period was not observed again. The cell voltage always decreased after H_2S was added, but regenerated to the initial level (±4 mV) after the H_2S was stopped. During the regeneration following the concentration of 100 ppm H_2S, the test was terminated unexpectedly. An overall cell voltage degradation excluding the periods under H_2S was not detectable and thus much similar to the reference test.

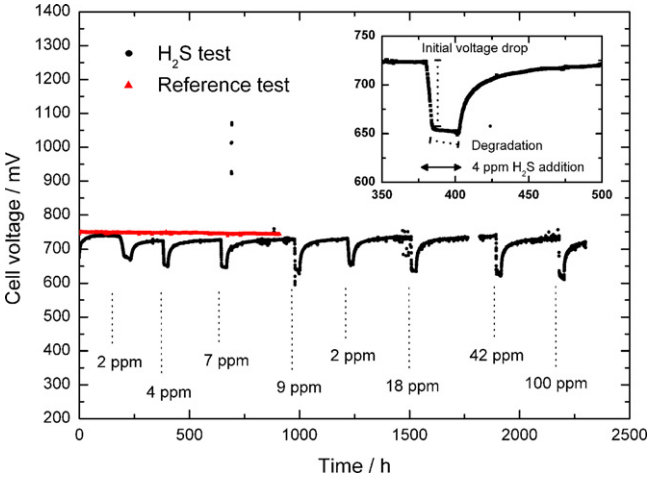

Fig. 2. The cell voltage development. The different H_2S amounts added are marked in the figure. The current load was 1 A cm^{-2} at a temperature of 850 °C for both tests. In the inserted figure the cell voltage development during the period with 4 ppm H_2S addition and evaluation parameters are shown. In the H_2S test an H_2/H_2O fuel mixture was used, at a FU of 70%. In the reference test an H_2/CO_2 fuel mixture was used, at a FU of 65%.

The effect of H_2S addition was evaluated using the initial cell voltage drop. The definition of this parameter is illustrated in the inserted figure in Fig. 2 and the results are shown in Fig. 3. The magnitude of the voltage drop increased sharply with increasing amounts of up to ∼10–20 ppm H_2S and to a smaller extent at larger concentrations. The error bars indicate the uncertainty of determining the exact starting and ending point of the initial voltage drop.

After the initial voltage drop, the cell voltage degraded at an almost constant rate (see insert in Fig. 2). Fig. 4 shows how this degradation rate depended on the H_2S concentration. The degradation rate during addition of H_2S increased with increasing H_2S concentration over the whole concentration range.

During the addition of H_2S, not only the cross-plane voltage (cell voltage), but also the in-plane voltages in the anode and cathode were recorded. These voltage values were measured at positions between the gas inlet and the gas outlet on the electrodes and are shown for the case of 2 ppm H_2S in Fig. 5. The in-plane voltage started to increase immediately after H_2S was added to the fuel. It went through a sharp peak during H_2S exposure and returned to a constant level (similar to that before the H_2S was added). This level remained constant until the H_2S was turned off. Then another peak was seen during the regeneration of the cell voltage. This time it evolved in the reverse direction and was much broader, however it rose again towards a constant level similar to the initial one. A similar behaviour was observed for the other concentrations of H_2S.

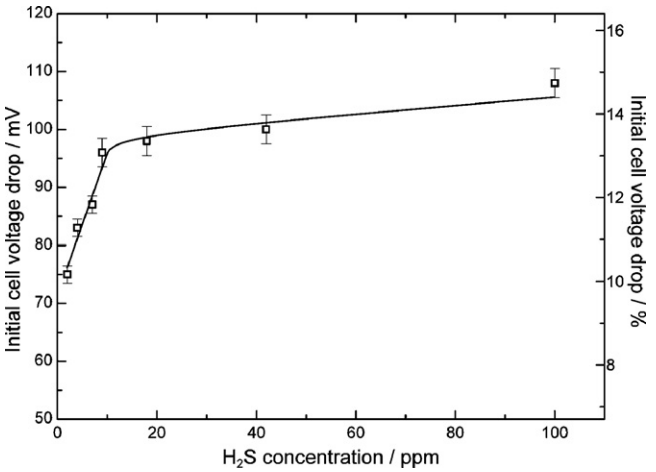

Fig. 3. The initial voltage drop as a function of the H_2S concentration. T = 850 °C, current load = 1 A cm^{-2}.

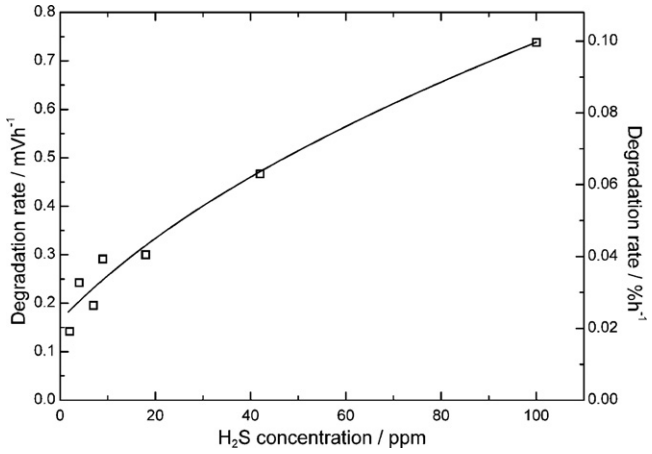

Fig. 4. Cell voltage degradation during addition of H_2S. $T = 850\,^{\circ}C$, current load = 1 A cm^{-2}.

The sign of the in-plane voltage was similar for the two electrodes. However, as seen in Fig. 5 they do not have the same magnitude. The anode in-plane voltage is twice as large as the cathode in-plane voltage.

The heights of the positive and negative peaks in the in-plane voltage in the anode were analysed as a function of the H_2S concentration (Fig. 6). The peak heights increased with increasing H_2S concentration until a plateau was reached at approximately 40 ppm H_2S. During the entire test period the in-plane voltage drifted. Error bars illustrating this drift are thus inserted in Fig. 6.

3.2. Impedance spectroscopy

Impedance of the SOFC was measured before, during and after each H_2S cycle, all under current load. To determine the most relevant times for recording impedance spectra the anode in-plane voltage was followed and impedance spectra were taken at the times of peaks and of constant levels. The development of the impedance was similar for all of the used H_2S concentrations. The case of 7 ppm H_2S addition is shown in Fig. 7 as example. The Nyquist plots show that the total internal resistance of the cell increased as H_2S was added to the fuel until the *constant level* in the in-plane voltage was reached. But it returned to the initial level when the H_2S addition was stopped, i.e. the cell voltage regenerated. The series resistance remained constant, only the polarization resistance changed.

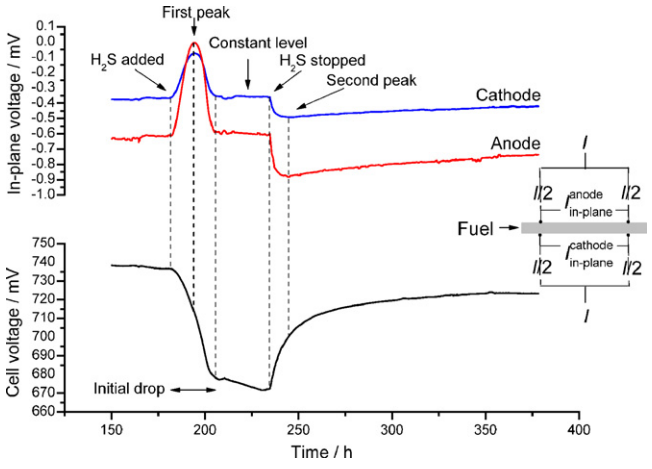

Fig. 5. The in-plane voltage development when 2 ppm H_2S was added to the fuel. $T = 850\,^{\circ}C$, current load = 1 A cm^{-2}.

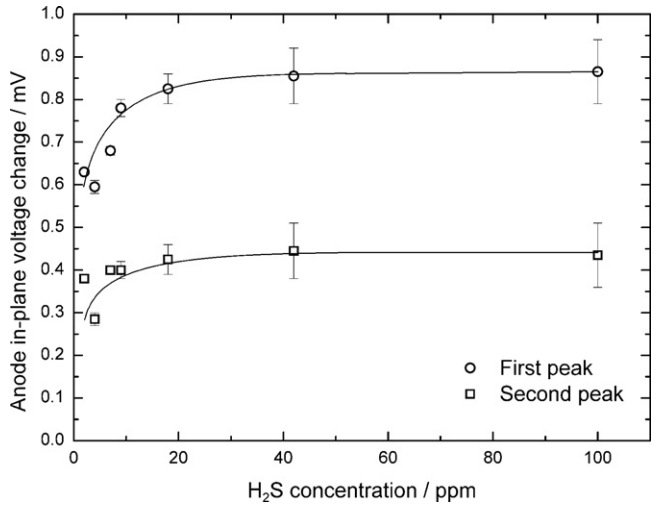

Fig. 6. The change in peak heights of the anode in-plane voltage for the first (positive) and second (negative) peak (see Fig. 5). $T = 850\,^{\circ}C$, current load = 1 A cm^{-2}.

In order to compare the performance after each portion of H_2S, the impedance spectra measured before each new addition of H_2S are shown in Fig. 8. The spectra have all approximately the same size and frequency range. Obviously, no permanent increase of cell resistance due to the addition of up to 42 ppm H_2S occurred.

ZView (*version* 2.8*d*) was used to analyse the impedance spectra. An equivalent circuit, which consisted of one inductance part, L, a series resistance, R_s, and three *R-CPE* elements ($R_1 + R_2 + R_3$) was used (the range of the resistances R_1, R_2 and R_3 and the fitted spectrum are indicated in Fig. 8 for the case before 2 ppm H_2S addition). This equivalent circuit has been found suitable for analysing the type of SOFC used in this study [27]. The analysis of the impedance spectra in Fig. 7 showed that the low-frequency arc (fitted by R_3) did not change significantly in size during the addition of H_2S. Instead the high frequency part (fitted by $R_1 + R_2$) stands for the change in internal resistance (Fig. 9).

To determine the exact frequency at which the impedance is affected most by the addition of H_2S, differential impedance analysis can be used [28]. Impedance spectra taken *before H_2S* introduction and at the *constant level*, i.e. during addition of H_2S, were

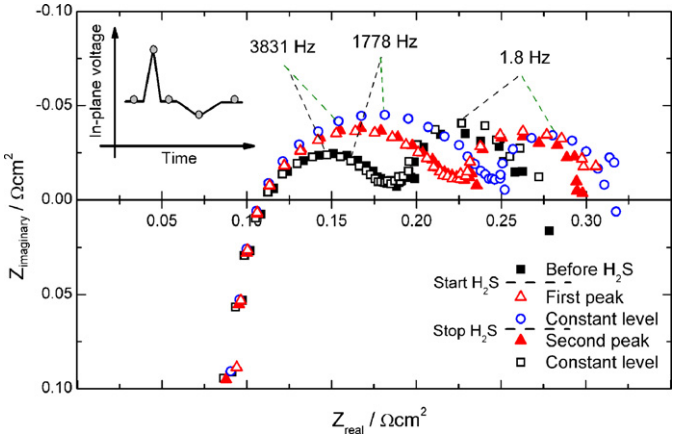

Fig. 7. Impedance spectra taken during the addition of 7 ppm H_2S to the fuel. The inserted figure shows when the impedance spectra were measured during the in-plane voltage development. The measurements at 3831 Hz, 1778 Hz and 1.8 Hz are marked, in order to show the development of the individual impedance arcs. $T = 850\,^{\circ}C$, current load = 1 A cm^{-2}.

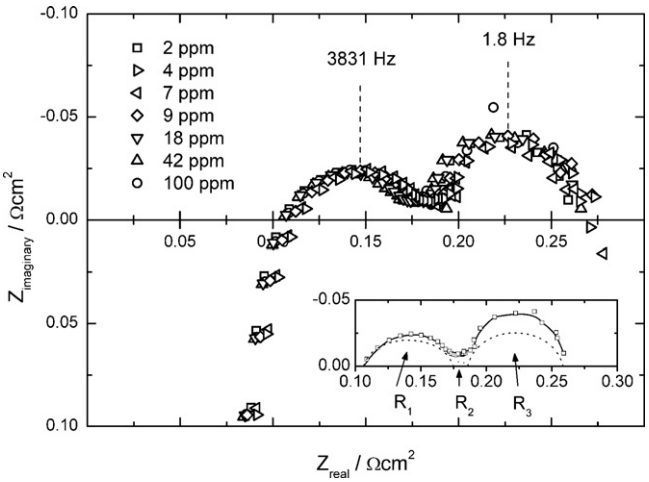

Fig. 8. Impedance spectra measured before each addition step of H_2S. The measurements at 3831 Hz, 1778 Hz and 1.8 Hz are marked, in order to show the development of the individual impedance arcs range of the resistances R_1, R_2 and R_3 and the fitted spectrum are indicated for the case of 2 ppm H_2S. T = 850 °C, current load = 1 A cm^{-2}.

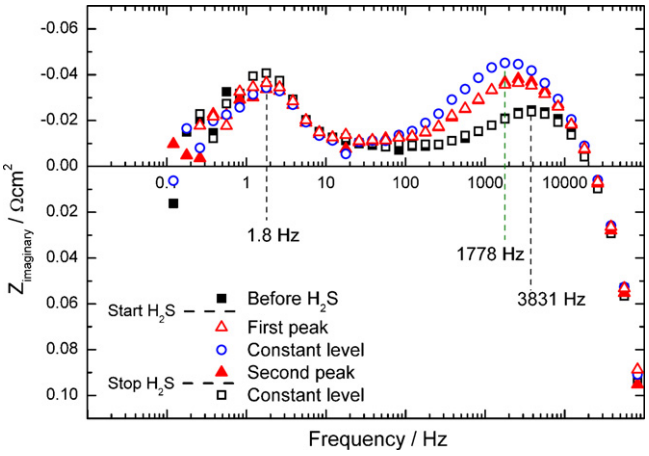

Fig. 9. The imaginary part of the impedance plotted as a function of frequency for the case of adding 7 ppm H_2S. The measurements at 3831 Hz, 1778 Hz and 1.8 Hz are marked, in order to show the development of the individual impedance arcs. T = 850 °C, current load = 1 A cm^{-2}.

compared. In the differential analysis the unit $\Delta\dot{Z}'(\omega_n)$ is calculated:

$$\Delta\dot{Z}'(\omega_n) \cong \frac{[Z'_B(\omega_{n+1}) - Z'_B(\omega_{n-1})] - [Z'_A(\omega_{n+1}) - Z'_A(\omega_{n-1})]}{\ln(\omega_{n+1}/\text{rad s}^{-1}) - \ln(\omega_{n-1}/\text{rad s}^{-1})} \quad (4)$$

where Z'_B is the real part of the *constant level* impedance spectrum and Z'_A is the real part of the impedance spectrum *before* H_2S, at the frequencyω. $\Delta\dot{Z}'(\omega_n)$ marks the frequencies at which differences in internal resistance between two given impedance spectra exist, in our case the frequencies at which the largest changes in the total internal resistance have taken place as a consequence of the H_2S addition. This is found to happen primarily at 1212 Hz (Fig. 10) for the studied H_2S concentrations 2 ppm, 4 ppm, 7 ppm, 18 ppm and 42 ppm. Furthermore, the magnitude of the change increased with increasing H_2S concentration.

4. Discussion

The addition of H_2S to a hydrogen fuel at 850 °C and 1 A cm^{-2} had two effects on the cell voltage (Fig. 2): an initial cell voltage drop and an almost constant cell voltage degradation, which was larger than during the periods without H_2S. A similar result has been reported in the literature [8,11]. Zha et al. [11] assigned the first voltage drop

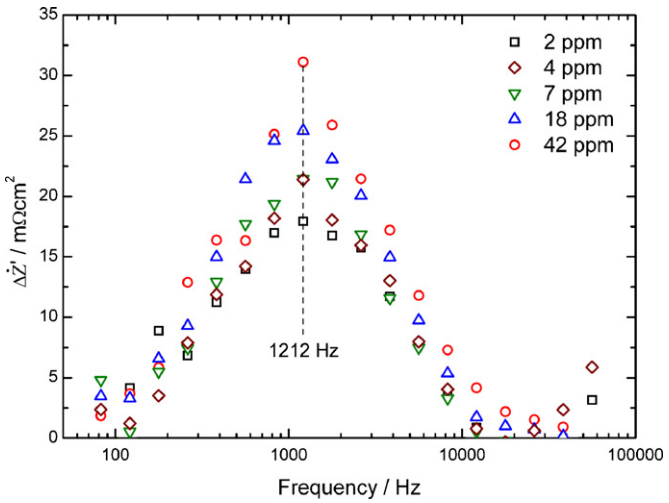

Fig. 10. Differential impedance analysis of spectra at "before H_2S" and at "constant level" for 2 ppm, 4 ppm, 7 ppm, 18 ppm and 42 ppm H_2S. T = 850 °C, current load = 1 A cm^{-2}.

to a rapid adsorption of S on the Ni surface, blocking the active sites for hydrogen adsorption and oxidation.

For all of the used concentrations of H_2S a detectable effect was seen on the cell voltage. This indicates that the lower concentration limit for a detectable effect of H_2S on the cell voltage for an SOFC of the type and with the test parameters used here is 2 ppm or below. Turning off the H_2S addition, however, the cell performance regenerated completely. The SOFC used here can thus tolerate H_2S exposures from 2 ppm to 100 ppm for a 24 h period in H_2 fuel. The magnitude of the initial voltage drop increased first sharply with increasing H_2S concentration until ~40 ppm (Fig. 3). A similar behaviour was observed for the change in the in-plane voltage (Fig. 6). A levelling off for both values occurred at larger H_2S concentrations, in particular for the in-plane voltage changes. Sasaki et al. [8] also observed a flattening out of the cell voltage drop, when increasing the H_2S concentration from 0 ppm to 20 ppm in an H_2 fuel for electrolyte supported SOFCs (Ni–YSZ anode) at a current load of 200 mA cm^{-2}, however at a much higher temperature of 1000 °C. The formation of the plateau may be related to the S-poisoning of the Ni anode catalysts. Bartholomew [2] reported that S adsorbs in different overlayers depending on the S/$Ni_{surface}$ ratios. S adsorbs selectively, i.e. adsorbs on the sites of lowest coordination number first, i.e. the most open structures bind S strongest. In the SOFC anode the Ni particle surfaces are a combination of different surface structures, which gives a large number of low coordinated sites. The initial cell voltage drop is thus a result of a fast chemisorption and therefore blocking of Ni sites most active for the electrochemical conversion of H_2. The magnitude of the drop is related to the number of blocked sites, i.e. the equilibrium coverage at a given H_2S concentration. The trends in Figs. 3 and 6 may thus be explained by "saturation" of one S-overlayer combination (represented by the solid line). At even higher H_2S concentrations (or maybe starting at 100 ppm) the initial voltage drop could thus increase again, due to a rearrangement of the S-overlayer. Increasing the temperature would decrease the effect of S on the performance and thus decrease the initial voltage drop.

In contrast to the immediate effect of H_2S, on the cell voltage, the degradation under exposure increased over the whole concentration range (2–100 ppm H_2S) (see Fig. 4). The origin of this degradation is not clear at the moment. Significant micro-structural changes, such as Ni-particle coarsening, do not seem very likely, as the degradation stops completely after the removal of H_2S from the fuel.

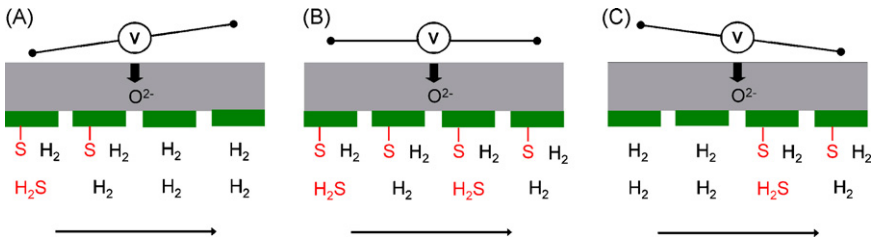

Fig. 11. Illustration of the S-poisoning of the SOFC anode (grey: electrolyte; green: Ni particles in anode; S: S-poisoning; arrows: fuel flow). (A) Ni particles partly covered (inlet); (B) homogeneous layer of S on the Ni particles; (C) S partly desorbed. (For interpretation of the references to color in this figure legend, the reader is referred to the web version of the article.)

Observing the cell voltage and the impedance spectra after stopping the H_2S addition (Figs. 7 and 8) an almost complete recovery of performance was obtained approximately 250 h after turning off the H_2S. The effect of H_2S on the electrochemical conversion can thus be regarded reversible. The main part of the regeneration happened within the first 50 h. This relatively quick performance recovery and the fact that it recovered completely, strongly indicate that the interaction of H_2S with the Ni catalyst was an adsorption reaction. This is further supported when considering the test conditions used in these studies (850 °C and 2–100 ppm H_2S) and taking previous results into consideration. Phase diagrams [19] show that an H_2S concentration well above 100 ppm at 850 °C is needed to form nickel sulfide and Raman spectroscopy studies support this statement [23]. However, a minor degree of nickel sulfide formation cannot be excluded.

Following from the previous discussions the shown regeneration of the cell performance is suggested to be due to S desorption. Adsorbed S species could react with H_2 from the fuel or O^{2-}-ions from the cathode–electrolyte (Reactions (5) and (6)). O^{2-}-ions were suggested to facilitate removal of adsorbed S by Cheng et al. [9], Zha et al. [11] and Rostrup-Nielsen et al. [12].

$$H_{2,g/ads} + S_{ads} \rightarrow H_2S_g \quad (5)$$

$$2O^{2-} + S_{ads} \rightarrow SO_{2,g} + 4e^- \quad (6)$$

Wang and Liu [29] used first-principles-based thermodynamic calculations to study desorption of S from a Ni surface and found that both H_2O and O_2 can be used as desorption agents. The concentrations of H_2O and O_2 must though not be too large (depending on the test parameters), as H_2O and O_2 may oxidise the Ni particles. In our tests, 4% H_2O was added to the fuel and the H_2O concentration increased, when the fuel moved towards the outlet part of the cell, as it is formed in the electrochemical conversion of H_2. H_2O is thus believed to have an influence on desorbing S from the Ni particles.

It must be remembered that the adsorption/desorption reactions are in equilibrium, which means that S is adsorbed and desorbed constantly due to the constant fuel flow. This gives an equilibrium coverage of S on the Ni particles, which depends on the fuel composition (concentration of H_2S and of desorption agent) and the operating parameters (temperature, current load, fuel utilization and cell polarization).

A change in the in-plane voltage is equal to a change of the current distribution within the electrode (from fuel inlet to outlet). This is illustrated in Fig. 5. Before adding H_2S to the H_2/H_2O fuel, the current I across the cell is divided equally between the inlet and outlet probes ($I/2$). The current running in-plane ($I_{in\text{-}plane}$) is thus close to 0. When H_2S is added to the fuel, a change of the in-plane voltage occurs ($I_{outlet} > I_{inlet}$ Fig. 5). The current distribution in the electrodes is changed in a way that part of the inlet $I/2$ current runs in-plane to the outlet $I/2$. This effect can be explained in terms of decrease of active sites due to S-passivation and *vice versa* when H_2S is stopped.

It is therefore suggested (illustration in Fig. 11) that H_2S enters the anode and adsorbs dissociatively on the Ni particles, starting at the inlet part of the anode. As a consequence the current distribution within the anode, and thus the anode in-plane voltage, change. When the anode is partly covered with S, the in-plane voltage is largest, i.e. the current distribution over the anode is most varied (*A* in Fig. 11 and *first peak* in Fig. 5). As the adsorption/desorption equilibrium is established, the in-plane voltage drops again, and reaches a constant level as a homogeneous layer covers the anode, i.e. the current is homogeneously distributed (*B* in Fig. 11 and *constant level* in Fig. 5). The degree of S coverage in this equilibrium situation depends on the fuel composition (concentration of H_2S and of desorption agent) and the operating parameters (temperature, current load, fuel utilization and cell polarization). As the effect of H_2S on the initial cell voltage drop and the peak heights of the in-plane voltage levels off after approximately 40 ppm, this concentration might reflect the amount of most active sites for H_2 oxidation at the anode/electrolyte interface. When the H_2S is turned off, the S on the Ni particles is desorbed after reaction with H_2 (and possibly O^{2-}-ions and H_2O). This desorption starts at the inlet, which leads to a difference of current distribution within the anode and therefore a change in the in-plane voltage. The reason for the smaller, broader, in-plane voltage change in this situation could be an indication for a slower desorption kinetics compared to the adsorption, i.e. the active sites bind S at a higher rate than release S. This would also explain the cell voltage development during the degradation/regeneration cycle (*C* in Fig. 11 and as *second peak* in Fig. 5).

Impedance spectroscopy under current load showed that the total internal resistance of the SOFC increased as H_2S was added to the fuel (the same effect was reported at OCV in the literature [11]) and reached a maximum at equilibrium coverage. Only the polarization resistance increased/changed whereas the series resistance remained constant. The adsorbed S species thus did not form an insulating layer, but poisoned the active sites for H_2 oxidation. The effect was completely reversible, as observed both with cell voltage and with impedance spectra in Figs. 7 and 8.

The changes of resistance happened primarily at the high frequency arc of the polarization resistance. These changes were characterized using differential impedance analysis. It was found that the main change in resistance happened at 1212 Hz. As S will poison the electrolyte/anode interface reactions, the 1212 Hz region can therefore be assigned to electrolyte/anode reactions for the type of SOFC and testing conditions used in this study.

The anode/electrolyte interface of the cell from the *H_2S test* and of a similar type of cell, which had not been exposed to H_2S (*Reference test*) were studied by electron microscopy. Comparing the Ni particle densities (the number of Ni particles within a 20 μm × 20 μm area adjacent to the anode/electrolyte interface, i.e. the active anode layer) on several positions, approximately similar values were found (25 ± 5 particles), see Fig. 12. There was a large uncertainty in determining the number of Ni particles, as smaller particles (below ~1 μm) were difficult to identify as Ni,

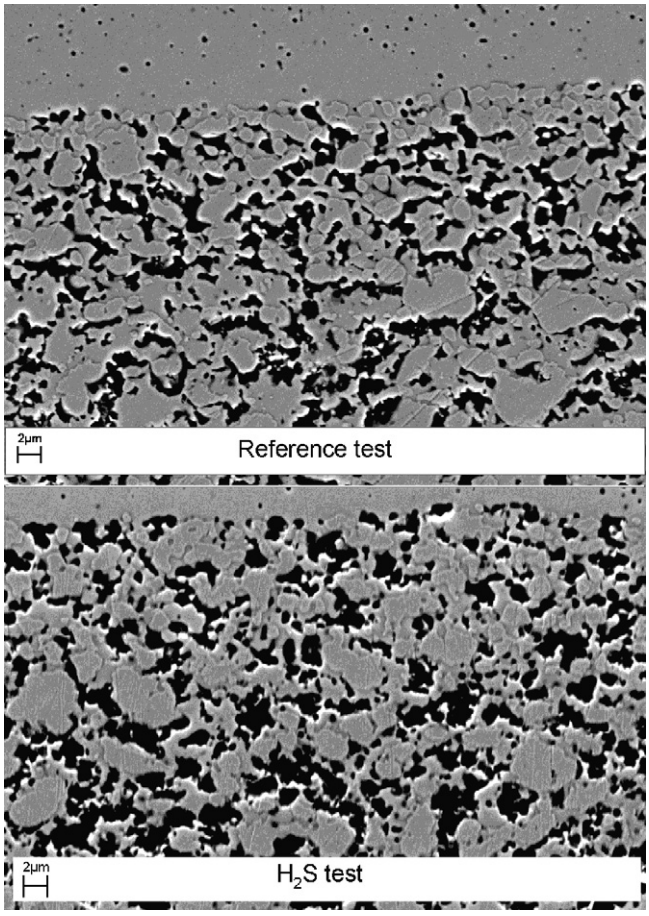

Fig. 12. Electron microscopy images of a reference (cell tested for long time at 850 °C without H_2S; top image) and the cell used in the H_2S test (bottom image). The images are oriented with the electrolyte on top and the anode below. A secondary electron detector and an acceleration voltage of 12 kV were used.

and due to particle agglomeration. However, it can be concluded that the short term exposure to H_2S under testing conditions did not seem to have a significant effect on the distribution of Ni. The only difference between the two images seemed to be a slightly larger porosity of the cell in the H_2S test. More analysis is necessary to confirm or dismiss this difference. No S-compounds, which could be related to the presence of H_2S in the fuel, were found in post-test EDS studies. However, it cannot be excluded that S-species were removed during shutdown of the test. Furthermore, the measurement resolution of the instruments used for post-test analysis could be a limiting factor. The measured parameters are only averages over the cell area. Local gradients may give the right conditions for nickel sulfide formation (e.g. different fuel flow or concentration).

5. Conclusions

In this article it has been demonstrated how H_2S affects the electrochemical performance of an anode-supported technological SOFC. H_2S in a H_2 fuel at 850 °C and 1 A cm^{-2} had a reversible effect on the electrochemical performance and cell voltage degradation rate in the concentration range between 2 ppm and 100 ppm H_2S admitted for 24 h periods. It was concluded that the poisoning effect of S was primarily due to chemisorption and thus blocking of Ni-particles and not a significant change of the microstructure of the anode or a formation of an insulating layer. The cell voltage degradation rate increased with increasing H_2S concentration, whereas there was no degradation in H_2S-free fuel under the used testing conditions. The S poisons the anode reversibly like a front and was reflected in a characteristic change of the in-plane voltage. The observed changes of the cell voltage, the in-plane voltage and the impedance at selected times showed that adsorption proceeds faster than desorption. Differential analysis of impedance spectra made it possible to identify the frequency of 1212 Hz at which S affects the total internal resistance of an SOFC, while the series resistance was not affected by H_2S at all. A forthcoming study will address the effect of H_2S in a biogas fuel where the poisoning effect on the electrochemistry as presented here will overlap with the poisoning effect on the reforming activity of the anode.

Nomenclature

SOFC	solid oxide fuel cell
CPO	catalytic partial oxidation
XRD	X-ray diffraction
SEM	scanning electron microscopy
EDS	energy dispersive spectroscopy
ASR	area specific resistance

Acknowledgement

We acknowledge the project “Effektiv konvertering af vedvarende energi vha. fastoxid-celler” under Det Strategiske Forskningsråds Programkomite for Energi og miljø, sagsnr. 2058-03-0014 for sponsoring this work.

References

[1] J.R. Rostrup-Nielsen, Catalytic Steam Reforming, Springer-Verlag, Berlin, 1984.
[2] C.H. Bartholomew, Applied Catalysis A: General 212 (2001) 17–60.
[3] C.H. Bartholomew, P.K. Agrawal, J.R. Katzer, Advances in Catalysis 31 (1982) 135–242.
[4] Y. Matsuzaki, I. Yasuda, Solid State Ionics 132 (2000) 261–269.
[5] J. Geyer, H. Kohlmüller, H. Landes, R. Stübner, Electrochemical Proceedings 18 (1997) 585–594.
[6] S. Primdahl, M. Mogensen, Electrochemical Society Proceedings 19 (1999) 530–540.
[7] Arnstein Norheim, Ph.D. thesis, 2005.
[8] K. Sasaki, K. Susuki, A. Iyoshi, M. Uchimura, N. Imamura, H. Kusaba, Y. Teraoka, H. Fuchino, K. Tsujimoto, Y. Uchida, N. Jingo, Journal of Electrochemical Society 153 (2006) A2023–A2029.
[9] Z. Cheng, S. Zha, M. Liu, Journal of Power Sources 172 (2007) 688–693.
[10] H. Kurokawa, T.Z. Sholklapper, C. Jacobson, L.C.D. Jonghe, S.J. Visco, Electrochemical and Solid State Letters 10 (2007) B135–B138.
[11] S. Zha, Z. Cheng, M. Liu, Journal of The Electrochemical Society 154 (2007) B201–B206.
[12] J.R. Rostrup-Nielsen, J.B. Hansen, S. Helveg, N. Christiansen, A.-K. Jannasch, Applied Physics A 85 (2006) 427–430.
[13] H. He, R.J. Gorte, J.M. Vohs, Electrochemical and Solid State Letters 8 (2005) A279–A280.
[14] J.P. Trembly, A.I. Marquez, T.R. Ohrn, D.J. Bayless, Journal of Power Sources 158 (2006) 263–273.
[15] A.I. Marquez, T.R. Ohrn, J.P. Trembly, D.C. Ingram, D.J. Bayless, Journal of Power Sources 164 (2007) 659–667.
[16] Y.M. Choi, C. Compson, M.C. Lin, M. Liu, Journal of Alloys and Compounds 427 (2007) 25–29.
[17] Y.M. Choi, C. Compson, M.C. Lin, M. Liu, Chemical Physics Letters 421 (2006) 179–183.
[18] M. Gong, X. Liu, J. Trembly, C. Johnson, Journal of Power Sources 168 (2007) 289–298.
[19] J.-H. Wang, M. Liu, Electrochemistry Communications 9 (2007) 2212–2217.
[20] J. Dong, Z. Cheng, S. Zha, M. Liu, Journal of Power Sources 156 (2006) 461–465.
[21] J.-H. Wang, Z. Cheng, J.-L. Brédas, M. Liu, The Journal of Chemical Physics 127 (2007) 214705-1–214705-8.
[22] Z. Cheng, H. Abernathy, M. Liu, The Journal of Physical Chemistry Letters C 111 (2007) 17997–18000.
[23] Z. Cheng, M. Liu, Solid State Ionics 178 (2007) 925–935.

[24] http://www.risoe.dk/Risoe_dk/Home/About_risoe/research_departments/ABF/Fuel_cells/manufacture.aspx, 2008.
[25] S. Ramousse, M. Menon, K. Brodersen, J. Knudsen, U. Rahbek, P.H. Larsen, ECS Transactions 7 (2007) 317–327.
[26] M. Mogensen, P.V. Hendriksen, High Temperature Solid Oxide Fuel Cells: Fundamentals, Design and Applications, Elsevier Ltd., Oxford, 2003.
[27] A. Hagen, M. Menon, R. Barfod, P.V. Hendriksen, S. Ramousse, P.H. Larsen, Fuel Cells 2 (2006) 146–150.
[28] S.H. Jensen, A. Hauch, P.V. Hendriksen, M. Mogensen, T. Jacobsen, Journal of the Electrochemical Society 154 (2007) B1325–B1330.
[29] J.-H. Wang, M. Liu, Journal of Power Sources 176 (2008) 23–30.